Exciton wave function, binding energy, and lifetime in InAs/GaSb coupled quantum wells

S. de-Leon and B. Laikhtman
Racah Institute of Physics, The Hebrew University, Jerusalem 91904, Israel
(Received 2 June 1999)

We studied theoretically excitons in narrow-coupled InAs/GaSb quantum wells where there is not any overlap between the InAs conduction subband and the GaSb valence subband. In this case, excitons do not exist in the equilibrium and the luminescence of pumped excitons can be observed. We calculated the exciton binding energy making use of the variational method. The resulting binding energy is around 4 meV. We also calculated the exciton lifetime for both radiative recombination and nonradiative recombination. Due to the unique band alignment of InAs/GaSb, the recombination can happen via two channels: first, mixing of the conduction band of InAs with the valence band of GaSb and second, electron tunneling from InAs conduction band to GaSb conduction band and hole tunneling from GaSb valence band to InAs valence band. The fastest recombination process is the radiative process in the second channel. The lifetime varies with the well widths from 45 ps for narrow wells to 400 ps for wider wells.

I. INTRODUCTION

Spatially indirect excitons in coupled quantum wells attract much interest recently both for possible applications in light-emitting devices and from the fundamental point of view, e.g., Bose Einstein condensation of excitons.[1–11] Confinement of excitons in quantum well increases their binding energy and spatial separation of electrons and holes increases the exciton lifetime.[12–16]

Most of the attempts to detect exciton Bose-Einstein condensation have been made in GaAs/$Al_xGa_{1-x}As$ coupled wells. Electrons and holes in this structure were pumped optically and in order to increase the exciton lifetime they were separated spatially by the application of an external electric field.[17–21] During the last years, a lot of work has been done also in InAs/GaSb heterostructures due to the unique band alignment of these materials. The bottom of the conduction band in bulk InAs lays below the top of the valence band in bulk GaSb, so there is an overlap between these bands. Due to this overlap electrons from the full valence band of GaSb are transferred to the empty conduction band of InAs leaving holes behind in the GaSb layer. As a result, a double layer is formed where electrons are confined in InAs while holes are confined in GaSb and the exciton state can be the ground state of the system.[8–10]

However, the advantage of excitons formation in equilibrium leads also to a difficulty in their observation. Equilibrium excitons do not luminesce and the only optical experiment that can be used is infrared absorption. A success in the exciton infrared absorption has been reported so far only in the presence of high-magnetic field.[8,10,22] All these results motivated us to consider narrow InAs/GaSb quantum wells, where excitons do not exist in equilibrium and therefore, can be detected by luminescence measurements.

In InAs/GaSb quantum wells the overlap between the ground electron subband in InAs and the ground hole subband in GaSb is reduced compared to the band overlap in bulk materials or even completely eliminated by the size quantization energy. Depending on their width, such coupled wells can be semimetallic, where there is an overlap between InAs conduction subband and GaSb valence subband or semiconducting, where there is no such overlap. If the gap in semiconducting InAs/GaSb heterostructure is larger than the exciton binding energy then excitons do not exist in equilibrium and they have to be pumped optically or with the help of an external electric field as in laser systems.[23,24]

The first problem that is considered in the present paper is the exciton binding energy and wave function in InAs/GaSb coupled quantum wells. Strictly speaking, this calculation is similar for equilibrium and nonequilibrium excitons, i.e., for semimetallic and semiconducting samples. The important parameters are, however, the widths of the wells.

An important parameter of nonequilibrium excitons that determines their luminescence intensity and affects the possibility of their Bose condensation is the recombination lifetime. And the second problem that we consider is the evaluation of the exciton lifetime in semiconducting InAs/GaSb coupled quantum wells.

The photon emission, however, is not the only recombination mechanism. An exciton can recombine also by emitting phonons. To compare the radiative and nonradiative (i.e., with phonon emission) recombination mechanisms we calculate the nonradiative lifetime with emission of one acoustic phonon. This mechanism may work in case of not-very-narrow quantum wells where the total energy of the exciton (the separation between the electron and hole levels minus the exciton binding energy) is not larger than the maximal acoustic phonon energy. The nonradiative lifetime appears to be by a few orders of magnitude larger than the radiative one. For this reason, we do not consider high-order processes with emission of more than one phonon or phonon and photon emission. We also do not consider recombination with optical phonon emission, which is relevant only in a very narrow exciton energy region.

In the next section, we present our model for the calculation of the exciton envelope function and the exciton lifetime. In Sec. III, we calculate the exciton wave function and it's binding energy using the variational principle, neglecting the penetration of electron and hole wave function between the wells. In Sec. IV, we describe this penetration, which is

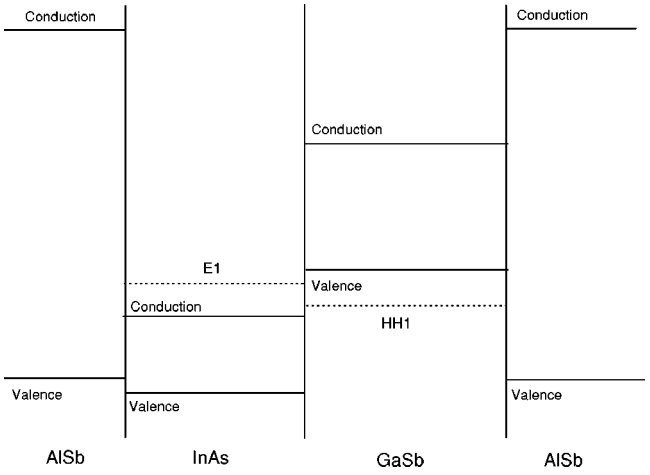

FIG. 1. InAs/GaSb-coupled quantum wells sandwiched between bulk samples of AlSb. The dashed line in the InAs layer in the first electron subband and the dashed line in the GaSb layer is the first heavy-hole subband. In this example the structure is semiconducting, i.e., there is no overlap between InAs first conduction subband and GaSb first valence subband.

necessary for the calculation of the exciton lifetime. In Sec. V, we obtain an expression for the exciton radiative lifetime. In Sec. VI, we calculate the recombination rate due to phonon emission. In the last section, we show numerical results for the lifetime in few cases and discuss them.

II. GENERAL DESCRIPTION OF THE MODEL

The physical system that we consider consists of two thin layers, one of InAs and the other of GaSb, sandwiched together in between bulk samples of a material that supplies high potential barrier for the carriers, e.g., AlSb (see Fig. 1). The offset between the InAs and the AlSb bulk conduction bands is about 2 eV, and between the InAs and the GaSb conduction bands is about 0.85 eV.[25,26] These barriers form a quantum well for electrons in the InAs layer. The offset between the GaSb and the AlSb bulk valence band is 0.4 eV, and between the GaSb and the InAs bulk valence band is 0.51 eV,[25,26] these barriers form a quantum well for holes in the GaSb layer.

In the calculation of the exciton wave function and binding energy we assumed that electrons and holes are confined separately in infinite quantum wells. The neglect of the carrier penetration between adjacent wells is justified as follows.

There are two penetration channels in this heterostructure. One is due to tunneling of electrons to the GaSb conduction band and tunneling of holes to the InAs valence band. This tunneling is weak due to the high-potential barriers.

Another penetration channel is due to the mixing of InAs conduction electrons and GaSb valence electrons. According to vertical transport experiments this mixing is also quite small. For example, in GaSb-InAs-GaSb heterostructure the current is evidently due to resonant tunneling, which indicates the formation of energy levels in the InAs layer due to size quantization.[27–30] Such levels can be formed only in the case of a weak penetration of carriers from InAs layer to GaSb.

Another simplification that we used in the calculation of the exciton structure is parabolic in-plane dispersion laws for both electrons and holes. This is a usual approximation for the electron spectrum, however, for the hole spectrum this approximation deserves a justification.

In quantum wells the degeneracy of the bulk valence band is lifted due to the size quantization. In a GaSb well of 100-Å width, the separation between the first subband (HH1) and the next level (LH1) is 45 meV. This separation is much larger than the exciton binding energy. In InAs/GaSb semiconducting heterostructures, the width of the GaSb well is typically smaller than 100 Å so the main contribution to the exciton envelop wave function comes from the first subband. The dispersion law of HH1 subband is nonparabolic and strongly anisotropic.[31,32] However, close to the subband edge the spectrum has a parabolic ''pocket'' with the mass significantly smaller than the bulk hole mass.[33–35] For infinite quantum well the ''pocket'' effective mass is given by the expression:[31,36]

$$\frac{1}{m_{\|}}=\gamma_1+\gamma_2-3\frac{\gamma_3^2}{\gamma_2}+3\frac{\gamma_3^2\sqrt{\gamma_1^2-4\gamma_2^2}}{\pi\gamma_2^2}\cot\left(\sqrt{\frac{\gamma_1-2\gamma_2}{\gamma_1+2\gamma_2}}\frac{\pi}{2}\right), \tag{2.1}$$

where γ_1, γ_2, and γ_3 are Luttinger parameters. For a small enough wave vector, $k\lesssim 1/L_v$ where L_v is the well width, the parabolic description is a good approximation of the spectrum. Our calculation shows that the exciton radius is by a few times larger than the width of the GaSb layer so the relevant wave vectors is smaller than $1/L_v$. Due to a finite depth of the well, the effective mass depends on the well width and the maximum of the corresponding correction to Eq. (2.1) reaches 25% for the well widths that we consider ($L_v=50$ Å). The exciton binding energy and wave function depend on the reduced mass, $\mu=m_e m_{\|}/(m_e+m_{\|})$. Here, the electron mass m_e is by approximately three times smaller than the hole mass $m_{\|}$ so that the resulting correction to μ is about 8% and we neglect it. So, for the calculation of the exciton structure it is possible to use the isotropic parabolic hole spectrum with the effective mass given by Eq. (2.1), which in GaSb is 0.08 m_0 (for $\gamma_1=11.8$, $\gamma_2=4.03$, and $\gamma_3=5.26$).

Another important point of the calculation of the exciton binding energy and wave function is that different dielectric constants in different layers of a heterostructure can strongly affect Coulomb interaction.[37–41] Dielectric constants of InAs and GaSb are 15.15 and 15.69, respectively and their difference can be neglected. The dielectric constant of AlSb is 12.04. The difference between the dielectric constant of the double layer and the cladding layers is important only at the distances larger than the width of the double layer. The exciton radius is a few times larger than the width of the double layer and one can expect that the effect of the dielectric constant difference of 20% is small. However, this is not obvious because the dependence of the exciton energy and the wave function on the dielectric constant can be stronger than linear (the energy of a bulk exciton is inverse proportional to the dielectric constant squared). To obtain the correct result and to estimate the effect of the different dielectric

constants, we carry out the calculation of the exciton binding energy and wave function for two cases. In the first one, we neglect the difference of the dielectric constants χ in different layers and assume $\chi=15$ all over the whole heterostructure. In the second case, we consider the dielectric constant $\chi=15$ inside the quantum wells and $\chi_1=12$ in the cladding layers.

In the second part of the paper, we calculate the radiative and nonradiative lifetime of the exciton. For this calculation, we have to go beyond the infinite wells approximation due to the following argument. Recombination is a transition of an electron from an initial state with the wave function $\Psi_{ei}(\mathbf{r})$ to a final state with the wave function $\Psi_{ef}(\mathbf{r})$ with emission of a photon or a phonon. The same process can be described as the annihilation of an electron from the state $\Psi_{ei}(\mathbf{r})$ and a hole from the state $\Psi_{hi}(\mathbf{r})=\Psi^*_{ef}(\mathbf{r})$. The matrix element of this process is

$$M=\int \Psi^*_{ef}(\vec{r})\mathcal{H}_{int}(\vec{r})\Psi_{ei}(\vec{r})d\vec{r}$$
$$=\int \delta(\vec{r}_e-\vec{r}_h)\mathcal{H}_{int}(\vec{r}_e)\Psi_{hi}(\vec{r}_h)\Psi_{ei}(\vec{r}_e)d\vec{r}_e d\vec{r}_h, \tag{2.2}$$

where $\mathcal{H}_{int}(\vec{r})$ is electron-photon or electron-phonon interaction Hamiltonian. When the electron and the hole are bound in exciton the product $\Psi_{hi}(\vec{r}_h)\Psi_{ei}(\vec{r}_e)$ is replaced by the exciton wave function $\Psi_{ex}(\vec{r}_e,\vec{r}_h)$, so that

$$M=\int \delta(\vec{r}_e-\vec{r}_h)\mathcal{H}_{int}(\vec{r}_e)\Psi_{ex}(\vec{r}_e,\vec{r}_h)d\vec{r}_e d\vec{r}_h. \tag{2.3}$$

It is important that the matrix element contains the exciton function (or its derivatives) at zero distance between electron and hole.[42] Electron and hole in InAs/GaSb-coupled quantum wells can appear at one point only if electrons from the conduction band of InAs pass to the GaSb conduction or valence band or if holes from the GaSb valence band pass to the InAs conduction or valence band. As we explained above, the penetration is small in all possible tunneling channels. That means that the tails of the electron wave function in GaSb and the tails of the hole wave function in InAs necessary for calculation of the matrix element (2.3) can be found with the help of the perturbation theory.

We realize that the accuracy of our calculation is limited. One of the fundamental reasons for such a limitation is that presently the exact form of the boundary conditions at interfaces between different materials is not known. We mean not only the boundary condition connecting conduction band wave function in InAs with the valence-band wave function in GaSb. Even the boundary conditions connecting wave functions of the conduction band of two different materials are not known exactly. In general, these boundary conditions contain an unknown parameter[43] that is usually taken to be equal unity without any reason except the simplification of calculations. This and similar reasons convinced us to chose in our calculations a simple model, which is easy to use. Indeed, any sophistication of the model makes the calculation much more difficult but do not improve its reliability because the uncertainty of the result comes from other sources (which is not sufficiently appreciated in many published calculations). E.g., we prefer to use perturbation theory even in the cases when the exact solution is known, for instance, in the calculation of the electron wave-function tail in the GaSb conduction band.

III. EXCITON ENVELOPE FUNCTION AND BINDING ENERGY

We consider a system with the following geometry: to the left, $-L_c<z<0$, there is an InAs layer that is a quantum well for electrons. To the right, $0<z<L_v$, there is a GaSb layer, which is a quantum well for holes. The layers are sandwiched in between a material that supplies high-potential barriers for both InAs electrons and GaSb holes, e.g., AlSb (see Fig. 1). In this section, we find the exciton envelope function and binding energy assuming complete confinement of the holes in the GaSb layer and the electrons in the InAs layer.

The Schrödinger equation for the exciton envelope function is

$$[H_{ce}+H_{vh}-V(\vec{r}_e,\vec{r}_h)]\Phi(\vec{r}_e,\vec{r}_h)=E\Phi(\vec{r}_e,\vec{r}_h), \tag{3.1}$$

where $\Phi(\vec{r}_e,\vec{r}_h)$ is the exciton envelope function, and

$$H_{ce}=-\frac{\hbar^2\nabla^2_{e,\|}}{2m_e}-\frac{\hbar^2}{2m_e}\frac{\partial^2}{\partial z_e^2}, \tag{3.2a}$$

$$H_{vh}=-\Delta-\frac{\hbar^2}{2m_\perp}\frac{\partial^2}{\partial z_h^2}-\frac{\hbar^2\nabla^2_{h,\|}}{2m_\|}. \tag{3.2b}$$

Here, $\nabla_{e,\|}$ and $\nabla_{h,\|}$ are the derivatives with respect to in-plane coordinates of electron, $\vec{r}_{e,\|}$, and hole, $\vec{r}_{h,\|}$, respectively. $\Delta\approx150$ meV is the energy difference between the bottom of the conduction band in bulk InAs and the top of the valence band in bulk GaSb. $m_e=0.026m_0$ is the electron effective mass in InAs, $m_\perp=0.27m_0$ and $m_\|=0.08m_0$ are the perpendicular and parallel to the layer plane GaSb heavy-hole effective masses. The electron-hole Coulomb interaction, $V(\vec{r}_e,\vec{r}_h)$, in the case of the same dielectric constants χ in the quantum wells and the cladding material is

$$V(\vec{r}_e,\vec{r}_h)=\frac{e^2}{\chi\sqrt{(z_e-z_h)^2+(\vec{r}_{e,\|}-\vec{r}_{h,\|})^2}}. \tag{3.3}$$

In the case when the dielectric constant χ_1 in the cladding layers is different from the dielectric constant χ in the quantum wells, the solution of the Poisson equation will result in

$$V(\vec{r}_e,\vec{r}_h)=\frac{2\pi e^2}{\chi}\int\frac{d^2k}{(2\pi)^2kg}e^{-i\vec{k}\vec{r}_\|}[t^2e^{-k(L_v+L_c)}e^{k(z_h-z_e)}$$
$$+2st\cosh k(z_h+z_e+L_c-L_v)$$
$$+s^2e^{k(L_v+L_c)}e^{-k(z_h-z_e)}], \tag{3.4}$$

where $\vec{r}_\|=\vec{r}_{e,\|}-\vec{r}_{h,\|}$, $t=1-(\chi_1/\chi)$, $s=1+(\chi_1/\chi)$, and

$$g=s^2e^{k(L_v+L_c)}-t^2e^{-k(L_v+L_c)}. \tag{3.5}$$

As it has already been mentioned, for numerical calculations we take $\chi=15$ and $\chi_1=12$.

The boundary conditions for the unperturbed problem, i.e., two infinite quantum wells are

$$\Phi(\vec{r}_e,\vec{r}_h)|_{z_e=-L_c}=\Phi(\vec{r}_e,\vec{r}_h)|_{z_e=0}=0, \tag{3.6a}$$

$$\Phi(\vec{r}_e,\vec{r}_h)|_{z_h=L_v}=\Phi(\vec{r}_e,\vec{r}_h)|_{z_h=0}=0. \tag{3.6b}$$

To simplify the solution of the Schrödinger equation we assume that the quantization energy in z direction is much larger than the in-plane kinetic energy and the Coulomb energy. This assumption is confirmed by the result of the calculation. So, in the leading order Eq. (3.1) is reduced to

$$\left(-\frac{\hbar^2}{2m_e}\frac{\partial^2}{\partial z_e^2}-\Delta-\frac{\hbar^2}{2m_\perp}\frac{\partial^2}{\partial z_h^2}\right)\Phi(\vec{r}_e,\vec{r}_h)=E^{(0)}\Phi(\vec{r}_e,\vec{r}_h). \tag{3.7}$$

The solution to this equation is found by separation of variables

$$\Phi(\vec{r}_e,\vec{r}_h)=\psi_c(z_e)\psi_v(z_h)f(\vec{r}_{h,\|},\vec{r}_{e,\|}), \tag{3.8}$$

where $f(\vec{r}_{h,\|},\vec{r}_{e,\|})$ is an arbitrary function. ψ_c and ψ_v for the ground state are

$$\psi_c(z_e)=\sqrt{\frac{2}{L_c}}\sin k_e z_e, \tag{3.9a}$$

$$\psi_v(z_h)=\sqrt{\frac{2}{L_v}}\sin k_h z_h, \tag{3.9b}$$

for $-L_c<z_e<0$, $0<z_h<L_v$ and equal zero outside of these regions. Also, $k_e=\pi/L_c$, $k_h=\pi/L_v$, $E^{(0)}=E_c+E_v$, and

$$E_c=\frac{\pi^2\hbar^2}{2m_eL_e^2},\quad E_v=-\Delta+\frac{\pi^2\hbar^2}{2m_\perp L_v^2}. \tag{3.10}$$

To find the first order correction to the energy due to the electron-hole interaction we have to calculate the diagonal matrix element of the $\vec{r}_{h,\|}$ and $\vec{r}_{e,\|}$ dependent part of the Hamiltonian (3.1) between the functions $\psi_c\psi_v$. This calculation leads to an equation for $f(\vec{r}_{h,\|},\vec{r}_{e,\|})$. We factorize this function into a part that describes the in-plane exciton motion as a whole, and a part that describes the relative motion of the electron and the hole,

$$f(\vec{r}_{e,\|},\vec{r}_{h,\|})=\frac{e^{i\vec{K}_\|\vec{R}_\|}}{\sqrt{S}}\phi(\vec{r}_\|), \tag{3.11}$$

where S is the normalization area, $\vec{K}_\|$ is the exciton wave vector and

$$\vec{r}_\|=\vec{r}_{e,\|}-\vec{r}_{h,\|},\quad \vec{R}_\|=\frac{m_e\vec{r}_{e,\|}+m_\|\vec{r}_{h,\|}}{m_e+m_\|}. \tag{3.12}$$

The part that describes the exciton structure satisfies the equation

$$\left[-\frac{\hbar^2\nabla_\|^2}{2\mu}+V(L_c,L_v,\vec{r}_\|)+\varepsilon\right]\phi(\vec{r}_\|)=0, \tag{3.13}$$

where

$$V(L_c,L_v,\vec{r}_\|)=-\int_0^{L_v}dz_h\int_{-L_c}^{0}dz_e|\psi_c(z_e)|^2|\psi_v(z_h)|^2\times V(\vec{r}_e,\vec{r}_h), \tag{3.14}$$

and the eigenvalue of Eq. (3.1) is

$$E=E^{(0)}+\frac{\hbar^2K^2}{2M}-\varepsilon. \tag{3.15}$$

Here, $M=m_e+m_\|$.

The substitution of Eqs. (3.9) and (3.3) in Eq. (3.14) results in

$$V(L_c,L_v,\vec{r}_\|)=-\frac{16\pi^4e^2}{\chi L_cL_v}\int_0^\infty\frac{(1-e^{-kL_c})}{k(4\pi^2+k^2L_c^2)}\times\frac{(1-e^{-kL_v})}{k(4\pi^2+k^2L_v^2)}J_0(kr_\|)dk, \tag{3.16}$$

where $J_0(kr)$ is the Bessel function.

When we consider the different dielectric constants of the cladding materials and use Eq. (3.4) instead of Eq. (3.3), we get:

$$\begin{aligned}V(L_c,L_v,\vec{r}_\|)=-\frac{16\pi^2e^2}{\chi L_cL_v}\int_0^\infty&\frac{J_0(kr_\|)dk}{k(4\pi^2+k^2L_c^2)k(4\pi^2+k^2L_v^2)g}\\&\times\{t^2(1-e^{-kL_v})(1-e^{-kL_c})+s^2(e^{kL_c}-1)\\&\times(e^{kL_v}-1)+st[(e^{kL_v}-1)(1-e^{-kL_c})\\&+(1-e^{-kL_v})(e^{kL_c}-1)]\}.\end{aligned} \tag{3.17}$$

We are interested in the ground state of the exciton for which $\phi(\vec{r}_\|)$ depends only on the modulus of $\vec{r}_\|$. We find function $\phi(r)$ with the help of variational method. To obtain more confident results we made the calculation for a few trial functions. We chose them making use of the asymptotic behavior of the Coulomb potential. At a distance much larger than the width of the wells, $V=-e^2/\chi r$. That means that $\phi(r)$ falls off at large r as a simple exponent. So we took

$$\phi_1(r,\alpha)=\frac{1}{\sqrt{2\pi}\alpha}\exp\left\{-\frac{r}{2\alpha}\right\} \tag{3.18}$$

as the first trial function. At small r the Coulomb potential (3.16) goes to a constant (the confinement in the z direction leads to cutoff of the Coulomb potential at $r=0$, so that $V(0)\approx-(e^2/\chi L)2\ln 2$, for $L_c=L_v=L$). That is $\phi(r)$ can be expanded in powers of r^2 at small r. So as the second trial function we took

$$\phi_2(r)=\frac{1}{\sqrt{\pi}a}\exp\left\{-\frac{r^2}{2a^2}\right\}, \tag{3.19}$$

TABLE I. The values of the variational parameters, the exciton binding energies of the three trail functions and the rms of the third trail function (r_3) for two well widths.

L_v[Å]	L_c[Å]	r_0[Å]	b[Å]	a[Å]	α[Å]	r_3[Å]	ε_1 [meV]	ε_2 [meV]	ε_3 [meV]	E [meV]
50	80	121	137	323	165	359	2.93	2.77	3.00	36
60	60	113	135	318	162	352	3.02	2.83	3.09	118

that is quite often used in variational calculations. As the third trial function we took a function that satisfied both asymptotes,

$$\phi_3(r,b,r_0)=\frac{1}{\sqrt{2\pi b(b+r_0)}}\exp\left\{-\frac{\sqrt{r^2+r_0^2}-r_0}{2b}\right\} \tag{3.20}$$

(compare Refs. 44–47). α, a, r_0 and b in Eqs. (3.18)–(3.20) are variational parameters.

Relatively simple expressions for variational functionals in all three cases are presented in Appendix A. The values of the variational parameters are found from the minimization of these functionals. The results of the calculation for all three trial functions for two different well widths in the case of the Coulomb potential Eq. (3.3) are presented in Table I. There ε_i is the binding energy corresponding to the trial function ϕ_i and E was defined in Eq. (3.15). To get an understanding of an overall width of the wave function, we presented in Table I also the root mean square (rms) radius of the third trial function $\phi_3(r)$ that is calculated according to

$$r_3^2=2b\frac{3b(b+r_0)+r_0^2}{b+r_0}. \tag{3.21}$$

For both well widths the second trial function (the Gaussian one) gives the smallest binding energy, i.e., the worst approximation and the third trial function gives the largest binding energy, i.e., is the best approximation. Comparing our results for the binding energy with the results of Monte-Carlo study that were done for similar systems[48] we see that the binding energy scales are similar (about 3 meV).

The difference between the binding energies of all trial functions is not large but it is more pronounced in their shape and radius. In Fig. 2, we present the shape of the three different trail wave functions for the case $L_v=L_c\equiv L=60$ Å.

For the third trial function, we calculated the exciton binding energy also with the interaction potential (3.17) that includes the difference of dielectric constants in the barriers and the wells. The results are presented in Table II. The binding energy is larger by about 25% and the rms is smaller by about 10% since the attraction is stronger. We see that the correction due to the different dielectric constant is substantial for the binding energy and the exciton radius. In Fig. 3, the change in the shape of the wave function due to the different dielectric constant of the cladding material is presented. We see that the wave-function amplitude is increased near $r=0$ and that the tail decreases faster due to the smaller dielectric constant of the barriers.

To check the parabolic spectrum approximation for holes in GaSb we calculated the Fourier transform of the third trial wave function, ϕ_{3k} (see Appendix B) and compared the value $|\phi_{3k}|^2$ for $k=1/L_v$ with $|\phi_{30}|^2$. It appears that for the structures that we studied the ratio $|\phi_{3k}|^2/|\phi_{30}|^2$ is smaller than 10^{-3}.

Finally, we compare the quantization energies in the well with the binding energy to justify the approximation that was made in the transition from Eqs. (3.1) to (3.7) and (3.13). The separation between the first and the second levels in the InAs well is about 490 meV and in GaSb well is about 80 meV, both are well above the binding energy.

IV. PENETRATION OF ELECTRONS AND HOLES TO THE NEIGHBORING WELLS

In this section, we will calculate the tails of the electron wave function in the GaSb quantum well and of the hole wave function in the InAs quantum well that are necessary for the calculation of the transition rate matrix element.

We treat the penetration of the wave function into the neighboring well with the help of perturbation theory. We have to distinguish here between two different parameters of the perturbation theory. The first one, the ratio of the exciton

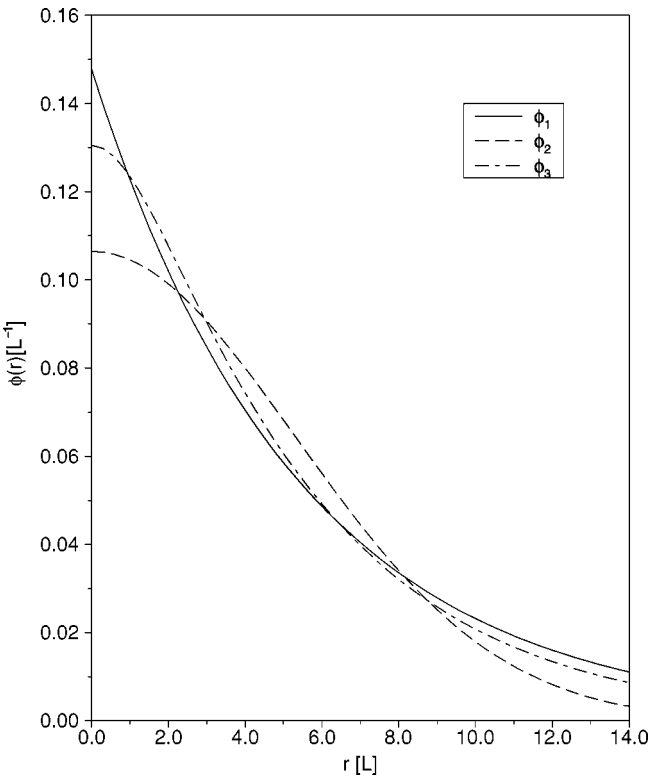

FIG. 2. The three trial functions of the relative coordinates in the case $L_v=L_c\equiv L=60$ Å. r is presented in units of L and ϕ_i is multiplied by L for convenience.

TABLE II. The values of the variational parameters, the exciton binding energy and rms of trail function ϕ_3 calculated for different dielectric constants in quantum wells and cladding layers.

L_v[Å]	L_c[Å]	r_0[Å]	b[Å]	r_3[Å]	ε_3 [meV]
50	80	126	121	324	3.98
60	60	133	116	313	4.12

binding energy to the quantization energy in the wells, has been used in the previous section and allowed us to factorize the exciton wave function to the form Eq. (3.8). In that section, we went beyond the leading order in this parameter and obtained Eq. (3.13) to calculate the in-plane exciton wave function $f(\vec{r}_{h,\|},\vec{r}_{e,\|})$. As soon as this wave function is known it is enough to work only in the leading order and neglect the in-plane kinetic energy and the electron-hole interaction compared to the quantization energy in the wells.

The second parameter of the perturbation theory describes the penetration between the wells. In the previous section, we used the boundary conditions (3.6) and neglected the penetration. This corresponds to the leading order of the perturbation theory. Now we have to go beyond the leading order and use the boundary conditions including the penetration. The corresponding step is the calculation of $\Phi(\vec{r}_e,\vec{r}_h)$ in the regions $0<z_e,z_h<L_v$ and $-L_c<z_e,z_h<0$ assuming that in the region $-L_c<z_e<0<z_h<L_v$ it is already known, Eqs. (3.8), (3.9), and (3.20). The pertubation parameter is the ratio of the energy shift due to the penetration to the quantization energy. However, to calculate the shift it is necessary to go to the second order of the perturbation theory that we are not going to do. Another way to estimate this parameter will be discussed at the end of Secs. IV A and IV B.

As it was mentioned in Sec. II, there are two penetration channels. In Sec. IV A, we calculate tails of the electron wave function in the valence band of GaSb and of the hole wave function in the conduction band of InAs. In Sec. IV B, we consider the penetration between conduction bands of these materials and between their valence bands.

A. Conduction-valence band mixing

To find $\Phi(\vec{r}_e,\vec{r}_h)$ in the regions $0<z_e,z_h<L_v$ and $-L_c<z_e,z_h<0$ we solve the Schrödinger equation in these regions and use boundary conditions that allow penetration between the quantum wells instead of Eq. (3.6). The Schrödinger equation that describes GaSb hole tunneling to the InAs conduction band and the Schrödinger equation that describes InAs electron tunneling to the GaSb valence band are similar to Eq. (3.7). The differences are that when an electron penetrates into the GaSb layer we need to replace H_{ce} with H_{ve}, and when a hole penetrates into the InAs layer we need to replace H_{vh} with H_{ch}, which are defined in the following way

$$H_{ve}=\Delta+\frac{\hbar^2}{2m_\perp}\frac{\partial^2}{\partial z_e^2}, \tag{4.1a}$$

$$H_{ch}=\frac{\hbar^2}{2m_e}\frac{\partial^2}{\partial z_h^2}, \tag{4.1b}$$

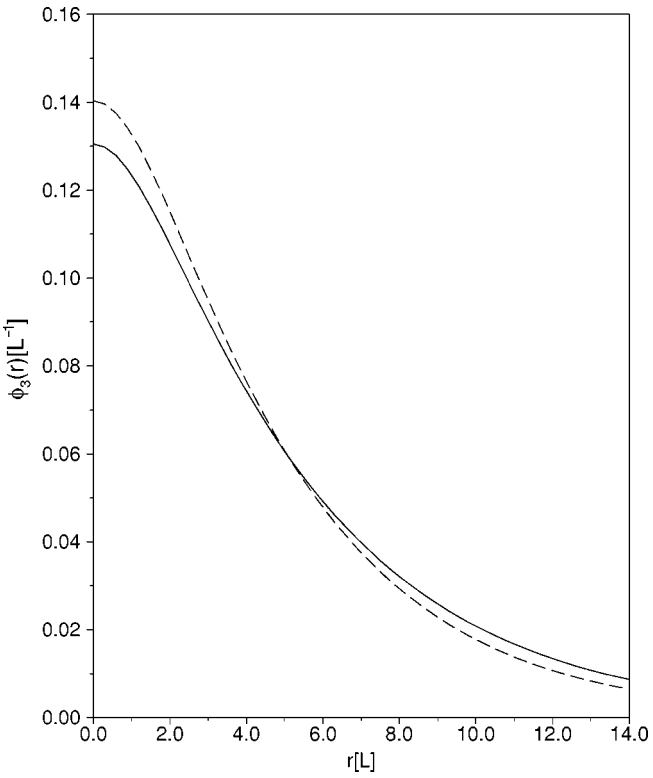

FIG. 3. The third trial function in the case $L_v=L_c\equiv L=60$ Å. The continuous line is for potential Eq. (3.3), i.e., dielectric constant $\chi=15$ everywhere. The dashed line is for the potential Eq. (3.4), i.e. $\chi=15$ in the wells, $\chi=12$ in the cladding materials.

where we neglect in-plane kinetic energy. As a result of this neglect in each of the regions $0<z_e,z_h<L_v$, and $-L_c<z_e,z_h<0$, the exciton wave function is factorized in a bit different way than in Eq. (3.8),

$$\Phi(\vec{r}_e,\vec{r}_h)=\psi_c(z_e)\psi_v(z_h), \tag{4.2}$$

$\psi_c(z_e)$ and $\psi_v(z_h)$ depend on $\vec{r}_{e,\|}$ and on $\vec{r}_{h,\|}$ as on parameters. The function $\psi_c(z_e)$ in the region $-L_c<z_e<0$, and the function $\psi_v(z_h)$ in the region $0<z_h<L_v$ are defined in Eq. (3.9) while in the other regions these functions satisfy the equations

$$\left(\Delta+\frac{\hbar^2}{2m_\perp}\frac{\partial^2}{\partial z_e^2}\right)\psi_c=E_c\psi_c,\ 0<z_e<L_v, \tag{4.3a}$$

$$\frac{\hbar^2}{2m_e}\frac{\partial^2\psi_v}{\partial z_h^2}=E_v\psi_v,\quad -L_c<z_h<0, \tag{4.3b}$$

where E_c and E_v are defined in Eq. (3.10). The solutions to these equations are

$$\psi_c(z_e)=C_e(\vec{r}_{e,\|},\vec{r}_{h,\|})\sin\kappa_e z_e+D_e(\vec{r}_{e,\|},\vec{r}_{h,\|})\cos\kappa_e z_e,\quad 0<z_e<L_v, \tag{4.4a}$$

$$\psi_v(z_h)=C_h(\vec{r}_{e,\|},\vec{r}_{h,\|})\sin\kappa_h z_h+D_h(\vec{r}_{e,\|},\vec{r}_{h,\|})\cos\kappa_h z_h,\quad -L_c<z_h<0, \tag{4.4b}$$

where $\kappa_e=\sqrt{2m_\perp(\Delta-E_c)}/\hbar$ and $\kappa_h=\sqrt{-2m_eE_v}/\hbar^2$. Note that κ_e is real only when $E_c=\pi^2\hbar^2/2m_eL_c^2<\Delta$, and κ_h is real only when $E_v<0$, i.e., $\pi^2\hbar^2/2m_\perp L_v^2<\Delta$.

To find the value of the coefficients C_e, D_e, C_h, and D_h we need boundary conditions for the electron and hole envelope functions. The barrier for electrons and holes created by the cladding material is quite high and we neglect any penetration there. So, the boundary conditions at the interfaces with the cladding material remain unchanged, Eq. (3.6). We need just correct boundary conditions at the interface between the wells that allow a penetration across this interface. Such boundary conditions for electrons have been obtained in Ref. 49. For the perturbation calculation that we use only one of them is necessary and it has the form

$$\Phi|_{z_e\to+0}=\frac{a_2}{2}\sqrt{\frac{m_\perp}{m_e}}\left(\frac{\partial}{\partial x_e}+i\frac{\partial}{\partial y_e}\right)\frac{\partial\Phi}{\partial z_e}\bigg|_{z_e\to-0}. \quad (4.5)$$

Here, a_2 is a phenomenological parameter that is close to aL_v where a is the lattice constant. The appearance of the derivative with respect to x and y in Eq. (4.5) (see also Ref. 50) is the results of the symmetry limitations.

Equation (4.5) describes the mixing of electron states between InAs conduction band and GaSb valence band. To describe similar mixing of hole states we make use of the relation between electron and hole wave functions, $\psi_h(\vec{r})=\psi_e^*(\vec{r})$. With the help of Ref. 49 we have

$$\Phi|_{z_h\to-0}=-\frac{a_2}{2}\sqrt{\frac{m_e}{m_\perp}}\left(\frac{\partial}{\partial x_h}+i\frac{\partial}{\partial y_h}\right)\frac{\partial\Phi}{\partial z_h}\bigg|_{z_h\to+0}. \quad (4.6)$$

With the help of these boundary conditions we obtain

$$\Phi_1(\vec{r}_e,\vec{r}_h)=-\frac{k_ha_2}{\sqrt{L_cL_v}}\sqrt{\frac{m_e}{m_\perp}}\left(\frac{\partial f}{\partial x_h}+i\frac{\partial f}{\partial y_h}\right)\times\frac{\sin\kappa_h(z_h+L_c)}{\sin\kappa_hL_c}\sin k_ez_e,\quad -L_c<z_h,z_e<0, \quad (4.7a)$$

$$\Phi_1(\vec{r}_e,\vec{r}_h)=-\frac{k_ea_2}{\sqrt{L_cL_v}}\sqrt{\frac{m_\perp}{m_e}}\left(\frac{\partial f}{\partial x_e}+i\frac{\partial f}{\partial y_e}\right)\times\frac{\sin\kappa_e(z_e-L_v)}{\sin\kappa_eL_v}\sin k_hz_h,\quad 0<z_e,z_h<L_v. \quad (4.7b)$$

We use the notation Φ_1 for the tails of the exciton wave function resulting from the mixing of InAs conduction and GaSb valence bands, to distinguish them from the other tails obtained in the next subsection. If κ_e or κ_h are imaginary the sin containing it in Eq. (4.7) should be replaced by sinh.

To justify the perturbation theory with respect to the penetration across the interface we have to check that the energy shift due to the penetration is much smaller than the separation between the first and the second levels in the wells. The same estimate can be made also in another way. In the leading order of the perturbation theory the value of the wave function at the interface is zero. The boundary conditions (4.5) and (4.6) give nonzero values for the interface wave function. The ratio of these values to the values of the wave function in the middle of the wells also gives us the parameter of the perturbation theory. Such an estimate gives the parameter $\lambda_e=a_2^2k_e\kappa_e/b^2$ for the electron penetration and $\lambda_h=a_2^2k_h\kappa_h/b^2$ for the hole penetration where b is one of the parameters of wave function (3.20). The values of the parameters vary from $\lambda_e=0.004$, $\lambda_h=0.01$ ($L_v=50$ Å, $L_c=80$ Å) to $\lambda_e=0.07$, $\lambda_h=0.025$ ($L_v=120$ Å, $L_c=70$ Å).

B. Conduction-conduction and valence-valence band mixing

The results for the second channel are obtained in a similar way. Again, we have the factorization (4.2) where $\psi_c(z_e)$ in the region $-L_c<z_e<0$ and $\psi_v(z_h)$ in the region $0<z_h<L_v$ are defined in Eq. (3.9). In the other regions, these functions satisfy the equations

$$\left(U_c-\frac{\hbar^2}{2m_e^{\mathrm{GaSb}}}\frac{\partial^2}{\partial z_e^2}\right)\psi_c=E_c\psi_c,\quad 0<z_e<L_v, \quad (4.8a)$$

$$\left(U_v-\Delta-\frac{\hbar^2}{2m_h^{\mathrm{InAs}}}\frac{\partial^2}{\partial z_h^2}\right)\psi_v=E_v\psi_v,\quad -L_c<z_h<0, \quad (4.8b)$$

where $U_v=0.51$ eV is the offset between the InAs and GaSb valence bands, and $U_c=0.85$ eV is the offset between their conduction bands, $m_e^{\mathrm{GaSb}}=0.042m_0$ is the effective electron mass in GaSb and $m_h^{\mathrm{InAs}}=0.4m_0$ is the heavy-hole mass in InAs.

The energy offsets between the bands in the different layers present barriers for tunneling of electrons into the GaSb layer and holes into InAs layer. These barriers are so high that the wave functions fall off significantly under the barriers at the distance smaller than the widths of the layers. For this reason, we can neglect the finite widths of the barriers.

For the calculation of under the barrier functions we use perturbation theory. This means that we neglect the change due to the penetration under the barrier of the electron function in InAs well and of the hole function in the GaSb well. Then the only necessary boundary conditions at the interface between the layers are the relation between the normal derivatives,[43,51,35,52–55]

$$\frac{1}{m_e^{\mathrm{GaSb}}}\frac{d\psi_c(z_e)}{dz_e}\bigg|_{z_e\to+0}=\frac{1}{m_e}\frac{d\psi_c(z_e)}{dz_e}\bigg|_{z_e\to-0}, \quad (4.9a)$$

$$\frac{1}{m_\perp}\frac{d\psi_v(z_h)}{dz_h}\bigg|_{z_h\to+0}=\frac{1}{m_h^{\mathrm{InAs}}}\frac{d\psi_v(z_h)}{dz_h}\bigg|_{z_h\to-0}. \quad (4.9b)$$

The resulting exciton envelope function is

$$\Phi_2(\vec{r}_e,\vec{r}_h)=\frac{2}{\sqrt{L_cL_v}}\frac{k_h}{q_h}\frac{m_h^{\mathrm{InAs}}}{m_\perp}f(\vec{r}_{e,\parallel},\vec{r}_{h,\parallel})e^{q_hz_h}\sin k_ez_e,\quad -L_c<z_h,z_e<0, \quad (4.10a)$$

$$\Phi_2(\vec{r}_e,\vec{r}_h) = -\frac{2}{\sqrt{L_c L_v}}\frac{k_e}{q_e}\frac{m_e^{\mathrm{GaSb}}}{m_e} f(\vec{r}_{e,\parallel},\vec{r}_{h,\parallel}) e^{-q_e z_e}\sin k_h z_h, \quad 0<z_e,z_h<L_v, \tag{4.10b}$$

where

$$q_e = \sqrt{2m_e^{\mathrm{GaSb}}|U_c - E_c|/\hbar^2},$$

$$q_h = \sqrt{2m_h^{\mathrm{InAs}}|U_v - E_v - \Delta|/\hbar^2}.$$

We use the notation Φ_2 for the tails of the exciton wave function originated from conduction-conduction and valence-valence band mixing.

The approximation of the infinite widths of the barriers that has been used to obtain Eq. (4.10) is valid if $q_e L_v \gg 1$ and $q_h L_c \gg 1$. For the cases that we have checked we have $q_e L_v$ equals 4.5 ($L_v = 50$ Å, $L_c = 80$ Å) and 10.5 ($L_v = 120$ Å, $L_c = 70$ Å) and $q_h L_c$ equals 10.4 ($L_v = 60$ Å, $L_c = 60$ Å) and 13.7 ($L_v = 50$ Å, $L_c = 80$ Å). The check of the perturbation theory with respect to the penetration across the interface can be made in the same way as in the Sec. IV A. That is, we compare the interface values of the wave functions obtained from Eq. (4.10) with the values of the electron wave function in the middle of InAs well and the hole wave function in the middle of GaSb well. This gives the parameter $g_e = (m_e^{\mathrm{GaSb}}/m_e)/q_e L_c$ for the electron penetration and $g_h = (m_h^{\mathrm{InAs}}/m_\perp)/q_h L_v$ for the hole penetration. For the well widths that we have considered we have g_e around 0.3 and g_h in the range 0.06–0.15.

V. RADIATIVE RECOMBINATION TIME OF EXCITON

The radiative recombination rate (the inverse recombination time) is calculated according to the Fermi golden rule when the interaction with the photon is $-(e/m_0 c)\vec{A}\vec{p}_e$ where m_0 is the free electron mass and $\vec{A}$ is the vector potential of light in the sample. The recombination rate is

$$\frac{1}{\tau_{rad}(K)} = \frac{4\pi^2 e^2}{m_0^2 V n^2}\Sigma_{q,s}\frac{1}{\omega_q}|\langle 0|\vec{\epsilon}_{\vec{q},s} e^{-i\vec{q}\vec{r}_e}\vec{p}_e|\Psi_{ex,\vec{K}}\rangle|^2 \times \delta(E-\hbar\omega_q). \tag{5.1}$$

Here $\vec{\epsilon}_{\vec{q},s}$ and ω_q are respectively the polarization vector and the frequency of a photon with the wave vector $\vec{q}$ and the polarization mode s. The refraction index is $n \approx 3.6$, $\vec{p}_e$ is the electron momentum operator, $\Psi_{ex,\vec{K}}$ is the wave function of the exciton with the wave vector $\vec{K}$ and V is the normalization volume. The matrix element in Eq. (5.1) is the same as Eq. (2.3) with specified interaction Hamiltonian.

The complete exciton wave function is a product of envelope function and Bloch functions. The Bloch functions that we need to consider depend on the tunneling channel. The coupling between the InAs conduction band and the GaSb valence band results in the following tails of the exciton complete wave function

$$\Psi_{ex}(\vec{r}_e,\vec{r}_h) = \begin{cases} \Phi_1(\vec{r}_e,\vec{r}_h)u_{c,\mathrm{InAs}}(\vec{r}_e)u_{c,\mathrm{InAs}}(\vec{r}_h), & -L_c<z_e,z_h<0, \\ \Phi_1(\vec{r}_e,\vec{r}_h)u_{v,\mathrm{GaSb}}(\vec{r}_e)u_{v,\mathrm{GaSb}}(\vec{r}_h), & 0<z_e,z_h<L_v, \end{cases} \tag{5.2}$$

where $u_{c,\mathrm{InAs}}(\vec{r})$ is Bloch function of InAs conduction band and $u_{v,\mathrm{GaSb}}(\vec{r})$ is Bloch function of GaSb valence band.

The conduction-conduction and the valence-valence band coupling results in the tails of the exciton complete wave function of the form

$$\Psi_{ex}(\vec{r}_e,\vec{r}_h) = \begin{cases} \Phi_2(\vec{r}_e,\vec{r}_h)u_{c,\mathrm{InAs}}(\vec{r}_e)u_{v,\mathrm{InAs}}(\vec{r}_h), & -L_c<z_e,z_h<0, \\ \Phi_2(\vec{r}_e,\vec{r}_h)u_{c,\mathrm{GaSb}}(\vec{r}_e)u_{v,\mathrm{GaSb}}(\vec{r}_h), & 0<z_e,z_h<L_v, \end{cases} \tag{5.3}$$

where $u_{v,\mathrm{InAs}}(\vec{r})$ is Bloch function of InAs valence band and $u_{c,\mathrm{GaSb}}(\vec{r})$ is Bloch function of GaSb conduction band.

When we calculate the matrix element we break the integration over the sample into the sum of integrals over unit cells. In the case of the wave function (5.2) when $\vec{p}_e$ operates on the Bloch function the integrals over unit cell give zero because two Bloch functions in each integral are identical and hence have the same parity. Therefore, the only nonzero contribution comes from derivatives of the envelope functions. In the case of Eq. (5.3), Bloch functions in each integral have different parity and hence nonzero contributions comes only from derivatives of the Bloch functions. The resulting matrix elements are

$$M_{ex1} \equiv \langle 0|\vec{\epsilon}e^{-i\vec{q}\vec{r}_e}\vec{p}_e|\Psi_{ex,\vec{K}}\rangle = -i\hbar\int e^{-i\vec{q}\vec{r}_e}\delta(\vec{r}_e-\vec{r}_h)\vec{\epsilon}\vec{\nabla}_e\Phi_1(\vec{r}_e,\vec{r}_h)d^3r_e d^3r_h, \tag{5.4a}$$

for the conduction-valence-band coupling and

$$M_{ex2} \equiv \langle 0|\vec{\epsilon}e^{-i\vec{q}\vec{r}_e}\vec{p}_e|\Psi_{ex,\vec{K}}\rangle = \vec{\epsilon}\vec{p}_{cv}^{\,\mathrm{InAs}}\int_{z<0} e^{-i\vec{q}\vec{r}_e}\delta(\vec{r}_e-\vec{r}_h)\Phi_2(\vec{r}_e,\vec{r}_h)d^3r_e d^3r_h + \vec{\epsilon}\vec{p}_{cv}^{\,\mathrm{GaSb}}\int_{z>0} e^{-i\vec{q}\vec{r}_e}\delta(\vec{r}_e-\vec{r}_h)\Phi_2(\vec{r}_e,\vec{r}_h)d^3r_e d^3r_h, \tag{5.4b}$$

for the conduction-conduction and valence-valence band coupling. Here,

$$\vec{p}_{cv}^{\,\mathrm{GaSb}} = \frac{1}{\Omega}\int_{cell} u_{v,\mathrm{GaSb}}^{\dagger}(\vec{r})\vec{p}u_{c,\mathrm{GaSb}}(\vec{r})d^3r, \tag{5.5a}$$

$$\vec{p}_{cv}^{\,\mathrm{InAs}} = \frac{1}{\Omega}\int_{cell} u_{v,\mathrm{InAs}}^{\dagger}(\vec{r})\vec{p}u_{c,\mathrm{InAs}}(\vec{r})d^3r, \tag{5.5b}$$

where Ω is the volume of a unit cell.

First, we find the radiative transition rate for valence-conduction coupling. With the help of the exciton envelope function calculated in the previous section, Eq. (4.7),

$$M_{ex1}=i\hbar\epsilon_z\frac{a_2}{\sqrt{L_cL_v}}\int d^2r_e d^2r_h\delta(r_{\|,e}-r_{\|,h})e^{-i\vec{q}\vec{r}_{\|,e}}$$
$$\times\left\{\left(\frac{\partial f}{\partial x_h}+i\frac{\partial f}{\partial y_h}\right)\epsilon_z k_h k_e\sqrt{\frac{m_e}{m_{h\perp}}}\right.$$
$$\times\int_{-L_c}^{0}\frac{\sin\kappa_h(z+L_c)}{\sin\kappa_h L_c}\cos k_e z dz+\left(\frac{\partial f}{\partial x_e}+i\frac{\partial f}{\partial y_e}\right)$$
$$\times\epsilon_z k_e\kappa_e\sqrt{\frac{m_{h\perp}}{m_e}}\int_0^{L_v}\frac{\cos\kappa_e(z-L_v)}{\sin\kappa_e L_v}\sin k_h z dz$$
$$+\left(\epsilon_x\frac{\partial}{\partial x_e}+\epsilon_y\frac{\partial}{\partial y_e}\right)\left(\frac{\partial f}{\partial x_h}+i\frac{\partial f}{\partial y_h}\right)k_h\sqrt{\frac{m_e}{m_{h\perp}}}$$
$$\times\int_{-L_c}^{0}\frac{\sin\kappa_h(z+L_c)}{\sin\kappa_h L_c}\sin k_e z dz$$
$$+\left(\epsilon_x\frac{\partial}{\partial x_e}+\epsilon_y\frac{\partial}{\partial y_e}\right)\left(\frac{\partial f}{\partial x_e}+i\frac{\partial f}{\partial y_e}\right)k_e\sqrt{\frac{m_{h\perp}}{m_e}}$$
$$\left.\times\int_0^{L_v}\frac{\sin\kappa_e(z-L_v)}{\sin\kappa_e L_v}\sin k_h z dz\right\}. \tag{5.6}$$

The photon wave length corresponding to this transition is a few orders of magnitude larger than the wells widths, (microns compared to hundred angstroms), so we assume that $\exp(-iq_z z)=1$ in the integrand.

It's more convenient to change the variables of the integration to the electron and hole center of mass coordinates $\vec{R}_\|$ and their relative coordinates $\vec{r}_\|$. Near the point $r_\|=0$ the potential is regular and hence the part of the wave function (3.11) depending on $r_\|$ behaves as $\phi(\vec{r}_\|)\approx\phi_0+\phi_1 r_\|^2$. So only the second derivatives of f are finite. As a result the terms in the right-hand side containing ϵ_z are proportional to K, which is relativistically small (due to the momentum conservation $K=q=\omega n/c$). The main contribution to terms containing ϵ_x and ϵ_y comes from the second derivatives of $\phi(\vec{r}_\|)$ with respect to $x_\|$ and $y_\|$.

After the substituting of the result in Eq. (5.1) and the summation over the in-plane momentum $\vec{q}_\|$, the transition rate for the conduction-valence-band mixing is

$$\frac{1}{\tau_{rad}(K)}=\frac{4\pi^2e^2}{m_0^2n^2}\frac{\hbar^2a_2^2}{L_cL_v}\Sigma_s\int\frac{dq_z}{2\pi\omega_{K,q_z}}\left|P_r\epsilon_x\frac{\partial^2\phi}{\partial x^2}\right.$$
$$\left.+iP_r\epsilon_y\frac{\partial^2\phi}{\partial y^2}+P_z\epsilon_z k_e(iK_x-K_y)\phi(0)\right|^2, \tag{5.7}$$

where the in-plane derivatives are taken at $r=0$, the photon frequency $\omega_{K,q_z}=c\sqrt{K^2+q_z^2}/n$ and

$$P_z=\frac{\kappa_e\sqrt{m_e m_{h\perp}}}{M}\int_0^{L_v}\frac{\cos\kappa_e(z-L_v)}{\sin\kappa_e L_v}\sin k_h z dz$$
$$-\sqrt{\frac{m_e}{m_{h\perp}}}\frac{k_h m_{h\|}}{M}\int_{-L_c}^{0}\frac{\sin\kappa_h(z+L_c)}{\sin\kappa_h L_c}\cos k_e z dz, \tag{5.8a}$$

$$P_r=k_h\sqrt{\frac{m_e}{m_{h\perp}}}\int_{-L_c}^{0}\frac{\sin\kappa_h(z+L_c)}{\sin\kappa_h L_c}\sin k_e z dz$$
$$+k_e\sqrt{\frac{m_{h\perp}}{m_e}}\int_0^{L_v}\frac{\sin\kappa_e(z-L_v)}{\sin\kappa_e L_v}\sin k_h z dz. \tag{5.8b}$$

Let x axis be directed along the vector K, so $\vec{q}$ is in the xz plane. One of possible polarization directions is perpendicular to the plane, i.e., along y direction $[\vec{\epsilon}=(0,1,0)]$ and the other is inside the plane xz. For the in-plane mode

$$\epsilon_x=\frac{q_z}{q_{ph}}=\frac{q_z}{\sqrt{K^2+q_z^2}}, \tag{5.9a}$$

$$\epsilon_y=0, \tag{5.9b}$$

$$\epsilon_z=\frac{K}{q_{ph}}=\frac{K}{\sqrt{K^2+q_z^2}}, \tag{5.9c}$$

and after the integration with respect to q_z we obtain the transition rate as the sum of contributions from the different polarization directions

$$\frac{1}{\tau_{rad}(K)}=\Gamma_x(K)+\Gamma_y(K)+\Gamma_z(K), \tag{5.10}$$

which are

$$\Gamma_z(K)=\frac{4\pi c_0^2e^2\hbar^3k_e^2}{m_0^2E^2n^2}|P_z|^2K^4|\phi(0)|^2\left(\frac{n^2E^2}{\hbar^2c^2}-K^2\right)^{-1/2}$$
$$\times\Theta\left(E-\frac{\hbar cK}{n}\right), \tag{5.11a}$$

$$\Gamma_x(K)=\frac{4\pi c_0^2e^2\hbar^3}{m_0^2E^2n^2}|P_r|^2\left|\frac{\partial^2\phi}{\partial x^2}\right|_{r=0}^2\left(\frac{n^2E^2}{\hbar^2c^2}-K^2\right)^{1/2}$$
$$\times\Theta\left(E-\frac{\hbar cK}{n}\right), \tag{5.11b}$$

$$\Gamma_y(K)=\frac{4\pi c_0^2e^2\hbar}{m_0^2c^2}|P_r|^2\left|\frac{\partial^2\phi}{\partial y^2}\right|_{r=0}^2\left(\frac{n^2E^2}{\hbar^2c^2}-K^2\right)^{-1/2}$$
$$\times\Theta\left(E-\frac{\hbar cK}{n}\right), \tag{5.11c}$$

where $c_0=a_2/\sqrt{L_cL_v}$.

Now we find the radiative transition rate in the second channel (valence-valence, conduction-conduction coupling).

Substituting $\Phi_2(\vec{r}_e,\vec{r}_h)$, Eq. (4.10), in Eq. (5.4b) we get the matrix element M_{ex2}. According to Eq. (5.1), after the summation with respect to the in-plane vector $q_\parallel$ we obtain Eq. (5.10) with

$$\Gamma_z(K)=\frac{4\pi e^2\hbar K^2\mathbf{d}_z^2}{m_0^2E^2n^2}|\phi(0)|^2\left(\frac{n^2E^2}{\hbar^2c^2}-K^2\right)^{-1/2}\times\Theta\left(E-\frac{\hbar cK}{n}\right), \tag{5.12a}$$

$$\Gamma_x(K)=\frac{4\pi e^2\hbar\mathbf{d}_x^2}{m_0^2E^2n^2}|\phi(0)|^2\left(\frac{n^2E^2}{\hbar^2c^2}-K^2\right)^{1/2}\Theta\left(E-\frac{\hbar cK}{n}\right), \tag{5.12b}$$

$$\Gamma_y(K)=\frac{4\pi e^2\mathbf{d}_y^2}{m_0^2\hbar c^2}|\phi(0)|^2\left(\frac{n^2E^2}{\hbar^2c^2}-K^2\right)^{-1/2}\Theta\left(E-\frac{\hbar cK}{n}\right), \tag{5.12c}$$

where

$$\vec{\mathbf{d}}=B_{\mathrm{InAs}}\vec{p}_{cv}^{\,\mathrm{InAs}}-B_{\mathrm{GaSb}}\vec{p}_{cv}^{\,\mathrm{GaSb}}, \tag{5.13a}$$

$$B_{\mathrm{InAs}}=\frac{2}{\sqrt{L_cL_v}}\frac{k_h}{q_h}\frac{m_h^{\mathrm{InAs}}}{m_\perp}\int_{-L_c}^{0}e^{q_hz}\sin k_ezdz, \tag{5.13b}$$

$$B_{\mathrm{GaSb}}=\frac{2}{\sqrt{L_cL_v}}\frac{k_e}{q_e}\frac{m_e^{\mathrm{GaSb}}}{m_e}\int_{0}^{L_v}e^{-q_ez}\sin k_hzdz. \tag{5.13c}$$

VI. NONRADIATIVE TRANSITION RATE

In this section, we calculate the exciton recombination rate due to emission of acoustic phonons with a wave vector much smaller than the inverse lattice constant. The calculation is similar to that in the previous section. However, as we will show below, the recombination time due to phonon emission contains only a contribution from the first tunneling channel, i.e., from the conduction-valence coupling.

The electron-phonon interaction is described by the following Hamiltonian:

$$\mathcal{H}_{ph}=\begin{cases}a_cu_{jj}, & z<0,\\ a_v(u_{xx}+u_{yy}+u_{zz})+\dfrac{b_v}{2}(u_{xx}+u_{yy}-2u_{zz}), & z>0,\end{cases} \tag{6.1}$$

where $a_c=5.8$ eV, $a_v=8.3$ eV, and $b_v=2$ eV are the deformation potential parameters of InAs and GaSb, respectively and

$$u_{jl}=i\Sigma_{q,s}\sqrt{\frac{\hbar}{2V\rho\omega_{q,s}}}q_je_{l,q,s}(a_{q,s}e^{i\vec{q}\vec{r}}-a_{q,s}^{\dagger}e^{-i\vec{q}\vec{r}}), \tag{6.2}$$

is the strain tensor. Here, $\omega_{q,s}=v_sq$ and $\vec{e}_{q,s}$ are respectively the frequency and the polarization vector of the phonon with the wave vector $\vec{q}$ and the branch s, v_s is the sound velocity and ρ is the lattice density ($\rho_{\mathrm{InAs}}=5.7$ g cm^{-3}, $\rho_{\mathrm{GaSb}}=5.6$ g cm^{-3}).

The inverse nonradiative lifetime for an exciton in the ground state as a function of the center of mass wave vector is

$$\frac{1}{\tau_{ph}(K)}=\frac{2\pi}{\hbar}\Sigma_{q,s}|\langle 1|\langle 0|\mathcal{H}_{ph}|\Psi_{ex,\vec{K}}\rangle|vac\rangle|^2\delta(E-\hbar\omega_{s,q}). \tag{6.3}$$

Here, $|vac>$ and $|1>$ are the initial and the final state of the phonon field, respectively.

Bloch wave functions of the conduction and valence bands have different parity and hence for small q the matrix element between them is zero. That is, the only contribution to the recombination rate comes from the first tunneling channel, i.e., valence-conduction band mixing, Eq. (5.2). According to Eq. (4.7) $\Phi_1(\vec{r},\vec{r})$ contains first derivatives of $f(\vec{r}_{e,\parallel},\vec{r}_{h,\parallel})$ at $\vec{r}_{e,\parallel}=\vec{r}_{h,\parallel}$. This function is a product of two factors, Eq. (3.11), and the first derivative of the factor $\phi(\vec{r}_\parallel)$ at zero argument equals zero. A nonzero contribution comes only from derivatives of the factor describing the exciton motion as a whole. This contribution is proportional to the small exciton wave vector K. So, after the substitution of $\Phi_1(\vec{r},\vec{r})$ in Eq. (6.3), and summation with respect the in-plane vector $\vec{q}$ we obtain

$$\begin{aligned}\frac{1}{\tau_{ph}}=&\frac{|c_{\mathrm{InAs}}|^2\hbar}{2\rho E}K^2|\phi(0)|^2\Sigma_s\int(\vec{q}\vec{e}_{s,q})^2a_c^2|I_{\mathrm{InAs}}(q_z)|^2\\&\times\delta(E-\hbar\omega_{s,q})dq_z\\&+\frac{|c_{\mathrm{GaSb}}|^2\hbar}{2\rho E}K^2|\phi(0)|^2\Sigma_s\int\left(\vec{q}\vec{e}_{q,s}\left(a_v+\frac{b_v}{2}\right)\right.\\&\left.-\frac{3b_v}{2}q_ze_{z,q,s}\right)^2|I_{\mathrm{GaSb}}(q_z)|^2\delta(E-\hbar\omega_{s,q})dq_z.\end{aligned} \tag{6.4}$$

Here, $\vec{q}_\parallel=\vec{K}$ and:

$$c_{\mathrm{InAs}}=\kappa_h\frac{2}{\sqrt{L_cL_v}}\frac{a_2}{2}\sqrt{\frac{m_e}{m_{h\perp}}}\frac{m_{h\parallel}}{M},$$

$$c_{\mathrm{GaSb}}=-\kappa_e\frac{2}{\sqrt{L_cL_v}}\frac{a_2}{2}\sqrt{\frac{m_{h\perp}}{m_e}}\frac{m_e}{M}, \tag{6.5a}$$

$$I_{\mathrm{InAs}}(q_z)=\int_{-L_c}^{0}e^{-iq_zz}\sin k_ez\frac{\sin\kappa_h(z+L_c)}{\sin\kappa_hL_c}dz, \tag{6.5b}$$

$$I_{\mathrm{GaSb}}(q_z)=\int_{0}^{L_v}e^{-iq_zz}\sin k_hz\frac{\sin\kappa_e(z-L_v)}{\sin\kappa_eL_v}dz. \tag{6.5c}$$

In InAs only the longitudinal phonons contribute to the recombination rate and $(\vec{q}\vec{e}_{l,q})^2=q^2=K^2+q_z^2$. In GaSb both

longitudinal and transverse phonons contribute to the product $q_z e_{z,q,t}$. We assume that $\vec{K}=K_x\vec{x}$, hence $\vec{q}$ is in the xz plane. There are two transverse modes, one is perpendicular to the xz plane and does not contribute to $q_z e_{z,q,t}$. The other mode is in the plane xz, we get for it $(q_z e_{z,q,t})^2=K^2q_z^2/q^2$.

The resulting transition rate for the ground state is

$$\frac{1}{\tau_{ph}(K)}=\Gamma_{\mathrm{InAs}}(K)+\Gamma_{\mathrm{GaSb},l}(K)+\Gamma_{\mathrm{GaSb},t}(K), \quad (6.6)$$

where

$$\Gamma_{\mathrm{InAs}}(K)=\frac{|c_{\mathrm{InAs}}|^2}{2\rho}K^2|\phi(0)|^2a_c^2\left(\frac{\pi q_z}{L_c\ \sin\kappa_hL_c}\right)^2\frac{1}{E\ v_{\mathrm{InAs},l}}$$
$$\times\frac{4\kappa_h^2q_z^2(\cos L_cq_z+\cos\kappa_hL_c)^2+(\sin\kappa_hL_c(\kappa_h^2+q_z^2-(\pi/L_c)^2)+2\kappa_hq_z\ \sin q_zL_c)^2}{[(\pi/L_c+\kappa_h)^2-q_z^2]^2[(\pi/L_c-\kappa_h)^2-q_z^2]^2}, \quad (6.7a)$$

$$\Gamma_{\mathrm{GaSb},l}(K)=\frac{|c_{\mathrm{GaSb}}|^2}{2\rho}K^2|\phi(0)|^2\left[\frac{\pi q_z(a_v-b_v)}{L_v\ \sin\kappa_eL_v}\right]^2\frac{1}{E\ v_{\mathrm{GaSb},l}}$$
$$\times\frac{4\kappa_e^2q_z^2(\cos L_vq_z+\cos\kappa_eL_v)^2+(\sin\kappa_eL_v(\kappa_e^2+q_z^2-(\pi/L_v)^2)+2\kappa_eq_z\ \sin q_zL_v)^2}{[(\pi/L_v+\kappa_e)^2-q_z^2]^2[(\pi/L_v-\kappa_e)^2-q_z^2]^2}, \quad (6.7b)$$

$$\Gamma_{\mathrm{GaSb},t}(K)=\frac{|c_{\mathrm{GaSb}}|^2}{2\rho}K^2|\phi(0)|^2\left(\frac{3\pi Kb_v}{4L_v\ \sin\kappa_eL_v}\right)^2\frac{1}{E\ v_{\mathrm{GaSb},t}}$$
$$\times\frac{4\kappa_e^2q_z^2(\cos L_vq_z+\cos\kappa_eL_v)^2+(\sin\kappa_eL_v(\kappa_e^2+q_z^2-(\pi/L_v)^2)+2\kappa_eq_z\ \sin q_zL_v)^2}{[(\pi/L_v+\kappa_e)^2-q_z^2]^2[(\pi/L_v-\kappa_e)^2-q_z^2]^2}. \quad (6.7c)$$

Here, we used the approximation $E/\hbar v_s=q=\sqrt{q_z^2+K^2}\approx q_z$ since $K\ll q_z$.

VII. DISCUSSION

In this section, we present the numerical results for the exciton wave function, the binding energy and the recombination lifetime. We made extensive calculations only for the trail function which gave the maximal binding energy, $\phi_3(r)$, Eq. (3.20). The results are given in Table III.

To understand a qualitative picture, we considered a few structures with different well widths of both wells. The difference of dielectric constants in quantum wells and cladding layers is taken into account in the calculation. First of all, we see that the wave function and the binding energy depend mainly on the average distance between electron and hole that is determined by sum of the well widths L_c+L_v. For a larger sum the exciton binding energy is smaller and the exciton radius is larger. If we keep this sum constant and vary the difference L_c-L_v the wave function parameters and the binding energy nearly do not change (see results for $L_c+L_v=140$ Å). The accuracy of the absolute values of the calculated parameters is no more than three digits and we give more digits only to show their relative change due to the variation of L_c-L_v. The overall size of the wave function is characterized by the rms value of its radius r_3.

In Table III, we present the exciton radiative lifetime separately for the first (τ_{rad1}) and the second (τ_{rad2}) recombination channels at $K=0$. Since $\Gamma_z(0)=0$ in both channels the only contribution to the lifetime comes from $\Gamma_x(0)$, $\Gamma_y(0)$. For the evaluation of the microscopic matrix elements $\vec{p}_{cv}^{\,\mathrm{InAs}}$, $\vec{p}_{cv}^{\,\mathrm{GaSb}}$, Eq. (5.5), we followed Ref. 56. There the Kane model is used, which gives $p_{cv}=\sqrt{E_pm_0/2}$ and the values of E_p extracted from experiments are $E_p^{\mathrm{InAs}}=21.11$ eV and $E_p^{\mathrm{GaSb}}=22.88$ eV.[56]

The lifetime in the second channel appears by more than five orders of magnitude shorter than the lifetime in the first channel. Such a big difference results from two main reasons. The first is that the Bloch function changes much faster than the envelope wave function. As a result the dipole moment for the interband transition in the second channel is by about two orders of magnitude larger than the dipole moment for the intraband transition in the first channel. The second reason is that the amplitude of the envelope wave function at the interface in the second channel is much larger than that in the first channel. [A rough comparison of Eq. (4.7) with Eq. (4.10) gives the large parameter $1/q_ea$ or $1/q_ha$.] So, in spite of very short tunneling tails in the second channel this gives another order of magnitude to the matrix element.

The main contribution to the recombination rate in the second channel comes from the electron tunneling from the InAs quantum well to the conduction band of GaAs quantum well. Due to small electron mass compared to the hole mass the part of the matrix element Eq. (5.13a), which describes the hole tunneling to the InAs valence band ($B_{\mathrm{InAs}}\vec{p}_{cv}^{\,\mathrm{InAs}}$) is by an order of magnitude smaller than the part describing electron tunneling ($B_{\mathrm{GaSb}}\vec{p}_{cv}^{\,\mathrm{GaSb}}$).

The dependence of the lifetime on the well widths comes mainly from the confinement energy. In the recombination rate, Eqs. (5.12b) and (5.12c), this energy enters through the factors $\mathbf{d}_x^2/E$ and $\mathbf{d}_y^2/E$, respectively [due to the dependence

TABLE III. The results of the calculation for a few heterosturtures using the trail function ϕ_3. Here r_0 and b are the values of the wave-function parameters, r_3 is the rms, ϵ_3 is the exciton binding energy, E is the total exciton energy, and $\tau_{rad1}(0)$ and $\tau_{rad2}(0)$ are the radiative recombination times in the first and the second channel, respectively for zero exciton wave vector.

L_v[Å]	L_c[Å]	L_c+L_v[Å]	r_0	b	r_3[Å]	ε_3 [meV]	E [meV]	$\tau_{rad1}(0)$[sec]	$\tau_{rad2}(0)$[sec]
60	60	120	133	116	312	4.12	118	6×10^{-5}	6.6×10^{-11}
50	80	130	126	121	322	3.98	36	7×10^{-6}	4.5×10^{-11}
60	80	140	130.7	125.1	332.6	3.8528	26	4×10^{-6}	5.2×10^{-11}
65	75	140	134.3	124.4	332.0	3.8519	40	1×10^{-5}	7.5×10^{-11}
70	70	140	135.4	124.2	331.8	3.8516	57	2×10^{-5}	9.7×10^{-11}
75	65	140	135.8	124.1	331.7	3.8519	79	4×10^{-5}	1.2×10^{-10}
80	60	140	135.9	124.0	331.5	3.8528	106	8×10^{-5}	1.3×10^{-10}
120	70	190	158	151	402	3.47	45	5×10^{-5}	4×10^{-10}

of $\mathbf{d}_j^2$ on k_e, Eq. (5.13)]. E.g., if we compare the lifetimes for $L_v=80$ Å and $L_c=60$ Å with the lifetime for $L_v=60$ Å and $L_c=80$ Å, we see that the total energy E decreases by four times, from 106 meV to 26 meV. At the same time the electron confinement energy decreases only by about 1.6 times, from 243 to 153 meV. As a result τ decreases by 2.5 times.

As we discussed above, the nonradiative recombination may be important only for wide-enough wells where the total exciton energy is larger than the highest acoustic phonon energy in InAs and GaSb (about 29 meV). To check its importance we give one example of such a case, $L_v=60$ Å, $L_c=80$ Å where the total exciton energy is about 26 meV. The nonradiative lifetime is infinite for $K=0$ since the recombination rate vanishes at this point [see Eqs. (6.6) and (6.7)]. As K increases the recombination rate increases and the lifetime reaches the value of 0.007 s for $K=2\times10^6$ cm^{-1} and then it decreases again. At this large K vector the radiative process is impossible due to momentum conservation. Since the energy relaxation processes are usually much faster than the nonradiative recombination we believe that excitons with such high K vectors relax to lower energy first and then recombine with the emission of a photon.

Thus, we see that the radiative recombination in the second channel is the most important process that limits the exciton lifetime. Due to the fact that the main contribution to the recombination comes from electron tunneling from InAs to GaSb layer this lifetime can easily be increased if a thin AlSb layer is grown in between InAs and GaSb layers. As we mentioned in Sec. II, AlSb presents a $U=2$ eV potential barrier for InAs conduction electrons. The AlSb layer of the width d will add a factor of $\exp(-q_b d)$ to the electron wave function in GaSb conduction band, where $q_b=\sqrt{2m_e^{\mathrm{AlSb}}|U-E_c|}/\hbar$ and $m_e^{\mathrm{AlSb}}=0.33m_0$ is the electron mass in AlSb. The layer of 12 Å (two lattice constants) gives about $\exp(-q_b d)=0.01$. Such a barrier practically does not affect the Coulomb potential and reduces the recombination rate by four orders of magnitude. Actually, this reduction is overestimated because if the electron tunneling is completely suppressed the recombination is still possible due to hole tunneling. The AlSb layer does not affect much the hole tunneling because the barrier for holes that it presents is only of 0.4 eV, which is lower than the InAs potential barrier. But without the barrier the hole tunneling is about two orders of magnitude weaker than the electron one. So the actual reduction of the recombination rate due to the AlSb barrier is about two orders of magnitude.

VIII. CONCLUSIONS

We have calculated the exciton wave function, binding energy, and lifetime in InAs/GaSb semiconducting coupled quantum wells where exciton luminescence can occur. The resulting binding energy for the wells that we have considered is about 3.5-4 meV. The exciton radiative lifetime strongly depends on the wells widths and can reach hundreds of picoseconds. A thin AlSb layer in between InAs and GaSb can increase the lifetime by two orders of magnitude. The nonradiative lifetime appears to be a few orders of magnitude larger than the radiative one.

ACKNOWLEDGMENTS

We appreciate discussions with L. D. Shvartsman. The work was supported by The Israel Science Foundation, Grant No. 174/98.

APPENDIX A: BINDING ENERGY OF THE EXCITON IN THE VARIATION METHOD

Multiplying Eq. (3.13) by $\phi^*(r)$ and integrating by parts the kinetic energy we get

$$\varepsilon_1(\alpha)=\int\left[\frac{\hbar^2}{2\mu}|\nabla\phi_1(r,\alpha)|^2+V(r)|\phi_1(r,\alpha)|^2\right]d^2r, \quad \text{(A1a)}$$

$$\varepsilon_2(a)=\int\left[\frac{\hbar^2}{2\mu}|\nabla\phi_2(r,a)|^2+V(r)|\phi_2(r,a)|^2\right]d^2r, \quad \text{(A1b)}$$

$$\varepsilon_3(b,r_0)=\int\left[\frac{\hbar^2}{2\mu}|\nabla\phi_3(r,b,r_0)|^2+V(r)|\phi_3(r,b,r_0)|^2\right]d^2r. \quad \text{(A1c)}$$

Some of the integrations can be done analytically, which results in

$$\varepsilon_1(\alpha)=\frac{\hbar^2}{8\mu\alpha^2}-\frac{16\pi^4e^2}{\chi L_cL_v\alpha^3}\int_0^\infty\frac{[1-\exp(-kL_c)]}{k(4\pi^2+k^2L_c^2)}\frac{[1-\exp(-kL_v)]}{k(4\pi^2+k^2L_v^2)}\left(\frac{1}{\alpha^2}+k^2\right)^{-3/2}dk, \tag{A2a}$$

$$\varepsilon_2(a)=\frac{\hbar^2}{2\mu a^2}-\frac{16\pi^4e^2}{\chi L_cL_v}\int_0^\infty\frac{[1-\exp(-kL_c)]}{k(4\pi^2+k^2L_c^2)}\frac{[1-\exp(-kL_v)]}{k(4\pi^2+k^2L_v^2)}\exp\frac{-(k^2a^2)}{4}dk, \tag{A2b}$$

$$\varepsilon_3(b,r_0)=\frac{\hbar^2}{8\mu b^2}\left[1-\frac{r_0^2\Gamma(0,r_0/b)}{b(b+r_0)}\exp(r_0/b)\right]-\frac{16\pi^4e^2}{\chi L_cL_vb(b+r_0)}\exp(r_0/b)\int_0^\infty\frac{[1-\exp(-kL_c)]}{k(4\pi^2+k^2L_c^2)}\frac{[1-\exp(-kL_v)]}{k(4\pi^2+k^2L_v^2)}$$
$$\times\frac{1}{b}\left(\frac{1}{b^2}+k^2\right)^{-3/2}\left(1+r_0\sqrt{\frac{1}{b^2}+k^2}\right)\exp\left(-r_0\sqrt{\frac{1}{b^2}+k^2}\right)dk. \tag{A2c}$$

APPENDIX B: FOURIER TRANSFORM OF THE EXCITON WAVE FUNCTION

To justify the parabolic spectrum approximation for holes in GaSb it is necessary to check that the Fourier components of the exciton wave function at $k\sim 1/L_v$ are small. The Fourier transform of $\phi_3(r,b,r_0)$, Eq. (3.20) that we used in our calculation is

$$\phi_{3k}=\sqrt{\frac{8\pi br_0^2}{b+r_0}}\left[\frac{1}{1+4k^2b^2}+\frac{2b}{(1+4k^2b^2)^{3/2}}\right]\exp\left[-\frac{r_0}{2b}(\sqrt{1+k^2r_0^2}-1)\right]. \tag{B1}$$

[1] Y. Kuramoto and C. Horie, Solid State Commun. **25**, 713 (1978).
[2] S. Datta, M.R. Melloch, and R.L. Gunshor, Phys. Rev. B **32**, 2607 (1985).
[3] L.V. Keldysh, in *Bose-Einstein-Condensation*, edited by A. Griffin, D. W. Snoke, and S. Stringari (Cambridge, New York, 1994).
[4] I.V. Lerner and Y.E. Lozovik, Solid State Commun. **23**, 453 (1977); J. Phys. C **12**, L501 (1979).
[5] D. Paquet, T.M. Rice, and K. Ueda, Phys. Rev. B **32**, 5208 (1985).
[6] Y.E. Lozovik and V.I. Yudson, Pis'ma Zh. Éksp. Teor. Fiz. **22**, 556 (1976) [JETP Lett. **22**, 274 (1976)]; Solid State Commun. **19**, 391 (1976).
[7] X. Zhu, J.J. Quinn, and G. Gumbs, Solid State Commun. **75**, 595 (1990).
[8] X. Xia, X.M. Chen, and J.J. Quinn, Phys. Rev. B **46**, 7212 (1992).
[9] Y. Naveh and B. Laikhtman, Phys. Rev. Lett. **77**, 900 (1996).
[10] J.-P. Cheng, J. Kono, B.D. McCombe, I. Lo, W.C. Mitchel, and C.E. Stutz, Phys. Rev. Lett. **74**, 450 (1995).
[11] L.V. Butov and A.I. Filin, Phys. Rev. B **58**, 1980 (1998).
[12] E. Hanamura, Phys. Rev. B **38**, 1228 (1988).
[13] L.C. Andreani, F. Tassone, and F. Bassani, Solid State Commun. **77**, 641 (1991).
[14] D.S. Citrin, Phys. Rev. B **47**, 3832 (1993).
[15] R.C. Iotti and L.C. Andreani, Semicond. Sci. Technol. **10**, 1561 (1995).
[16] R.C. Iotti, L.C. Andreani, and M. Di Ventra, Phys. Rev. B **57**, R15 072 (1998).
[17] T. Fukuzawa, S.S. Kano, T.K. Gustafson, and T. Ogawa, Surf. Sci. **228**, 482 (1990).
[18] J.E. Golub, K. Kash, J.P. Harbison, and L.T. Florez, Phys. Rev. B **41**, 8564 (1990).
[19] J.A. Kash, M. Zachau, E.E. Mendez, J.M. Hong, and T. Fukuzawa, Surf. Sci. **263**, 502 (1992).
[20] J.E. Golub, K. Kash, J.P. Harbison, and L.T. Florez, Phys. Rev. B **45**, 9477 (1992).
[21] V. Negoita, D.W. Snoke, and K. Eberl, Phys. Rev. B **60**, 2661 (1999).
[22] J. Kono, B.D. McCombe, J.-P. Cheng, I. Lo, W.C. Mitchel, and C.E. Stutz, Phys. Rev. B **50**, 12 242 (1994); J. Kono, B.D. McCombe, J.-P. Cheng, I. Lo, W.C. Mitchel, and C.E. Stutz, *ibid.* **55**, 1617 (1997).
[23] I. Vurgaftman, J.R. Meyer, F.H. Julien, and L.R. Ram-Mohan, Appl. Phys. Lett. **73**, 711 (1998).
[24] W.W. Bewley, I. Vurgaftman, C.L. Felix, J.R. Meyer, C.H. Lin, D. Zhang, S.J. Murry, S.S. Pei, and L.R. Ram-Mohan, J. Appl. Phys. **83**, 2384 (1998).
[25] K.F. Longenbach, L.F. Luo, S. Xin, and W.I. Wang, J. Cryst. Growth **111**, 651 (1991).
[26] D.Z.-Y. Ting, E.T. Yu, and T.C. McGill, Phys. Rev. B **45**, 3583 (1992).
[27] J.R. Söderström, D.H. Chow, and T.C. McGill, Appl. Phys. Lett. **55**, 1094 (1989).
[28] L.F. Luo, R. Beresford, and W.I. Wang, Appl. Phys. Lett. **55**, 2023 (1989).
[29] K. Tiara, I. Hase, and H. Kawai, Electron. Lett. **25**, 1708 (1989).
[30] E.T. Yu, D.A. Collins, D.Z.-Y. Ting, D.H. Chow, and T.C. McGill, Appl. Phys. Lett. **57**, 2675 (1990); D.Z.-Y. Ting, E.T. Yu, D.A. Collins, D.H. Chow, and T.C. McGill, J. Vac. Sci. Technol. B **8**, 810 (1990).
[31] A.V. Chaplik and L.D. Shvartsman, Surf. Phys. Chem. Mech. **2**, 73 (1982) (in Russian); L.D. Shvartsman, Solid State Commun. **46**, 787 (1983).
[32] S. de-Leon, L. D. Shvartsman, and B. Laikhtman, Phys. Rev. B. **60**, 1861 (1999).
[33] A. Matulis and K. Piragas, Fiz. Tekh. Poluprovodn. **9**, 2202

(1975) [Sov. Phys. Semicond. **9**, 1432 (1976)].
[34] M.I. D'yakonov and A.V. Khaetskii, Zh. Éksp. Teor. Fiz. **82**, 1584 (1982) [Sov. Phys. JETP **55**, 917 (1982)].
[35] G. Bastard, Phys. Rev. B **24**, 5693 (1981).
[36] B. Laikhtman, R.A. Kiehl, and D.J. Frank, J. Appl. Phys. **70**, 1531 (1991).
[37] N.S. Rytova, Vestn. Mosk. Univ., Physics **3**, 30 (1967) (in Russian).
[38] A.V. Chaplik and M.V. Entin, Zh. Éksp. Teor. Fiz. **61**, 2496 (1971) [Sov. Phys. JETP **34**, 1135 (1972)].
[39] L.V. Keldysh, Pis'ma Zh. Éksp. Teor. Fiz. **29**, 716 (1979) [JETP Lett. **29**, 658 (1979)].
[40] E.A. Andryushin and A.P. Silin, Fiz. Tverd. Tela **22**, 2676 (1980) [Sov. Phys. Solid State **22**, 1562 (1980)].
[41] T. Ando, A.B. Fowler, and F. Stern, Rev. Mod. Phys. **54**, 437 (1982).
[42] R.J. Elliott, Phys. Rev. **108**, 1384 (1957).
[43] W.A. Harrison, Phys. Rev. **123**, 85 (1961).
[44] R.L. Greene, K.K. Bajaj, and D.E. Phelps, Phys. Rev. B **29**, 1807 (1984).
[45] T. Westgaard, Q.X. Zhao, B.O. Fimland, K. Johannessen, and L. Johnson, Phys. Rev. B **45**, 1784 (1992).
[46] Yutaka Takahashi, Yoshimine Kato, Satoru S. Kano, Susumu Fukatsu, Yasuhiro Shiraki, and Ryoichi Ito, J. Appl. Phys. **76**, 2299 (1994).
[47] J. Soubusta, R. Grill, P. Hlídek, M. Zvára, L. Smrčka, S. Malzer, W. Geißelbrecht, and G.H. Döhler, Phys. Rev. B **60**, 7740 (1999).
[48] E.G. Wang, Y. Zhou, C.S. Ting, J. Zhang, T. Pang, and C. Chen, J. Appl. Phys. **78**, 7099 (1995).
[49] S. de-Leon, B. Laikhtman, and L.D. Shvartsman, J. Phys.: Condens. Matter **10**, 8715 (1998); B. Laikhtman, S. de-Leon, and L.D. Shvartsman, Solid State Commun. **104**, 257 (1997).
[50] A. Fasolino and M. Altarelli, Surf. Sci. **142**, 322 (1984).
[51] D.J. BenDaniel and C.B. Duke, Phys. Rev. **152**, 683 (1966).
[52] S.R. White and L.J. Sham, Phys. Rev. Lett. **47**, 879 (1981); S.R. White, G.E. Margues, and L.J. Sham, J. Vac. Sci. Technol. **21**, 544 (1982).
[53] H. Kroemer and Q.-G. Zhu, J. Vac. Sci. Technol. **21**, 551 (1982); Q.-G. Zhu and H. Kroemer, Phys. Rev. B **27**, 3519 (1983).
[54] R. Lassing, Phys. Rev. B **31**, 8076 (1985).
[55] H.C. Liu, Superlattices Microstruct. **3**, 413 (1987); Appl. Phys. Lett. **51**, 1019 (1987).
[56] Gerald Bastard, *Wave Mechanics Applied to Semiconductor Heterostructures* (Halsted Press, New York, 1988), p. 49.